Available online at www.sciencedirect.com
SCIENCE DIRECT®
Mechanics of Materials 37 (2005) 407–425
MECHANICS OF MATERIALS
www.elsevier.com/locate/mechmat

# A variational method for non-linear micropolar composites

Gengkai Hu [a], Xiaoning Liu [a], Tian Jian Lu [b,*]

[a] Department of Applied Mechanics, Beijing Institute of Technology, Beijing 100081, PR China
[b] Department of Engineering, Cambridge University, Trumpington Street, Cambridge CB2 1PZ, UK

Received 9 December 2003; received in revised form 1 March 2004

**Abstract**

Built upon Ponte Castañeda's method for a Cauchy medium, a variational method for evaluating the effective non-linear behavior of micropolar composites is proposed. The same as for a Cauchy medium, it is shown that the proposed variational method can be interpreted as the secant moduli method based on second-order stress and couple stress moments. With simple examples, the interplay between material length parameters of a higher-order medium and its geometrical dimensions and/or material constants is highlighted. By using the new variational method, the influence of reinforcement size on the yielding and strain hardening of particulate composites is examined in a *simple and analytical* manner. The predictions agree well with existing experimental data for selected particulate metal matrix composite systems. The particle size effect is found to be more pronounced for shear loading and hard particles.


*Keywords:* Variational method; Particulate composite; Micromechanics; Non-linearity; Couple stress

## 1. Introduction

There has been rekindled interest in studying the size dependence of material properties, both experimentally and theoretically. The recent trend is driven largely by the practical need in the design, fabrication and characterization of miniaturized electronic, photonic and mechanical systems with length scales spanning from nanometers to submicrometers. Consequently, the applicability of classical continuum mechanics for ideal homogeneous materials in small structures has been subjected to acute scrutiny. For instance, for a thin film with only one or two layers of grains across the thickness, it is found that the homogenized material must have a non-local character in order to accurately describe the strain distribution in the film thickness (Haque and Saif, 2003).

In addition to the pronounced size dependence observed in macroscopically homogeneous solids, particle/fiber-reinforced metal matrix composites

* Corresponding author. Tel.: +44 1223 766316; fax: +44 1223 332662.
*E-mail addresses:* hugeng@public.bta.net.cn (G. Hu), tjl21@cam.ac.uk (T.J. Lu).

0167-6636/$ - see front matter © 2004 Elsevier Ltd. All rights reserved.
doi:10.1016/j.mechmat.2004.03.006

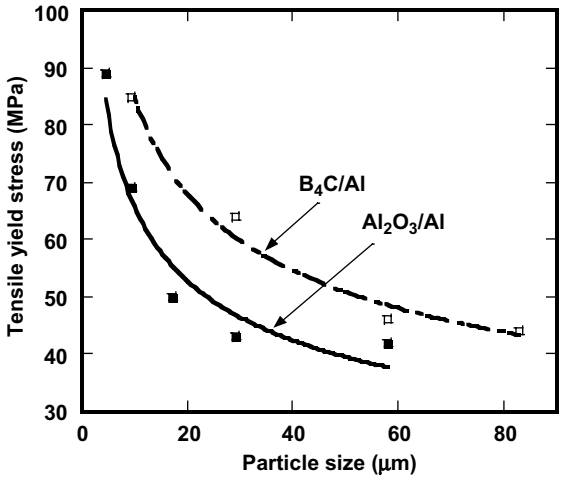


Fig. 1. Tensile yield stress (at 0.02% offset strain) of ceramic particle-reinforced aluminum matrix composite plotted as a function of particle size. Open and solid square symbols represent experimental data taken from Kouzeli and Mortensen (2002), whilst solid and dash lines represent curve-fitting.

also exhibit strong size dependent yielding/strengthening at the micron scale; see Fig. 1 plotted using the recent experimental data of Kouzeli and Mortensen (2002). However, in comparison with crystalline solids, theoretical studies on the size dependence of the non-linear overall properties of such composites are few. This paper aims to couple the higher-order, phenomenological elasticity and plasticity theory with Ponte Castañeda's variational method (Ponte Castañeda, 1991) to provide a simple analytical tool for predicting the non-linear behavior of particle-reinforced metal matrix composites as the reinforcement size is systematically decreased. We start by briefly reviewing the different length scales existing in composite materials, and the implications on higher-order non-local continuum theories.

### *1.1. Crystalline solids: length scales, size effects and higher-order plasticity theories*

Experimentally, it has been well established that, in a crystalline solid such as copper wires with diameter ranging from 12–170 μm (Fleck et al., 1994), nickel foils of thickness in the range of 12.5–50 μm (Stölken and Evans) and 0.1–0.5 μm thick aluminum films (Haque and Saif, 2003), the yield stress and strain hardening are strongly dependent upon the interplay amongst the characteristic geometric size of the material $L$ (e.g., film thickness), the internal geometric length scale $D$ (e.g., grain or void size), and the plasticity length scale $l$ characterizing, say, the gradient of plastic strains due to geometrically necessary dislocations. When $L \approx D \approx l \sim 1$ μm, the material becomes harder than its bulk counterpart, and the hardening/strengthening increases with the further decrease of $L$.

Theoretically, the current consensus is that a higher-order theory is necessary in order to capture and predict the experimentally observed size dependence (Fleck and Hutchinson, 2001). Whenever a high-order stress measure and the associated higher-order strain are introduced in addition to the classical Cauchy stresses and strains, one or more material length scales arise naturally due to dimensional consistency. From the continuum mechanics point of view, to include the non-local nature of the material into a continuum formulation, extra degrees of freedom (e.g., strain gradients and microrotations) must be introduced: such a non-local Cauchy medium will be referred to as the higher-order continuum in the following. In this paper, the Cauchy medium means that any material point in such medium can be considered as infinitesimally small, and any surface of such material element transmits only force. The higher-order continuum theory is introduced to describe more accurately the structural response of the material. According to different length scale conditions, different homogenization strategies should be adopted (Forest et al., 1999; Hu et al., 2004), as summarized in Table 1.

There exist different classes of higher-order plasticity theories, some phenomenological and some mechanism-based. The phenomenological theory is popular due to its simplicity, the representative being the strain gradient plasticity of Fleck and Hutchinson (1993), and its subsequent refinements/variations (e.g., Fleck and Hutchinson, 2001; Gao et al., 1999a,b; Chen and Wang, 2001). The Fleck–Hutchinson theory is built essentially upon the general framework of couple stress theory (see, e.g., Toupin, 1962; Midlin, 1964; Erin-

Table 1
Continuum models for different length scale conditions

| Continuum model | Length scale condition | | Homogenized continuum |
|---|---|---|---|
| Cauchy medium | $L \gg R$ | $D \gg l$ | Cauchy medium |
| | $L \gg D$ | $D \gg d$ | |
| Higher-order medium | $l \gg b$ | $D \approx l \sim 1$ μm | |
| | | $D \approx d$ | |
| Cauchy medium | $L \approx R$ | $D \gg l$ | Higher-order medium |
| | $L \approx D$ | $D \gg d$ | |
| Higher-order medium | $l \gg b$ | $D \approx l \sim 1$ μm | |
| | | $D \approx d$ | |

$L$ = structural dimension, $d$ = constituent (e.g., precipitate) size, $R$ = size of representative volume element, $b$ = dislocation spacing, $D$ = inhomogeneity (e.g., grain, particle) size, $l$ = (elastic or plastic) material length scale.

gen, 1968), as well as the classical $J_2$ deformation and flow theory of plasticity. The original version of the Fleck–Hutchinson theory contains only one length parameter $l_2$ associated with the rotation gradient, which may lead to erroneous predictions for cases where the stretch gradient is dominant (e.g., void growth, cavitation, crack-tip fields and indentation). A second length parameter $l_1$ linked with the stretch gradient is subsequently introduced (Fleck and Hutchinson, 2001), and its validity verified against experimental measurements. For metals, $l_1 = 0.2$–$0.5$ μm is typically one order of magnitude shorter than $l_2 = 2$–$5$ μm (Stölken and Evans, 1998; Fleck and Hutchinson, 2001). [1]

There are several different length scales at play in a real material (which is intrinsically heterogeneous). The classical phenomenological theory of plasticity ignores the microstructural details of the material, treating it as a homogenized Cauchy continuum. The underlying assumption of the homogenization is that $L \gg D$ and $L \gg l$ such that the homogenized Cauchy medium is equivalent to the original microheterogeneous material in terms of overall (effective) properties; until recently, a further assumption made, often implicitly, is that $D \gg l$. This is in general realized by introducing a representative volume element (RVE) whose size, $R$, gives an intermediate length scale between the structure and the local inhomogeneity (Nemat-Nasser and Hori, 1993), with $L \gg R \gg D$ and $L \gg R \gg l$ assumed. In other words, $R$ is small in macroscale but large in comparison with 'molecular' dimensions. In reality, there may exist another sub-microscopic geometric length $d$ which represents the size of inhomogeneities (constituents) within a grain of a crystalline solid. Although often not explicitly expressed, the fundamental assumption of classical continuum mechanics is $D \gg d$, as illustrated in Fig. 2a.

The various length scales of a microheterogeneous material may be differentiated into two main types. The first type includes $L$, $R$, $D$ and $d$, which represent separately macro, meso, micro and submicroscale geometric dimensions. The second type includes the material length parameter $l$ at the microscopic scale, which comes into play only when the deformation is such that non-negligible (elastic and plastic) strain gradients are induced: it may therefore be viewed as a representation of the wavelength of local stress and strain fluctuations, and as such it may depend upon the corresponding geometrical length scale such as $D$ and also, most likely, upon material constants since deformation and its gradients under stressing are involved. In classical continuum mechanics, the stress and strain wavelengths have the same order of magnitude as the structural length scale $L$, and hence $L$ may also be interpreted as a (global) material length parameter. As summarized in Table 1

[1] The most general Fleck–Hutchinson theory contains a third length parameter, $l_3$ but its influence is only of secondary consequence in all the practical cases that have hitherto been studied.

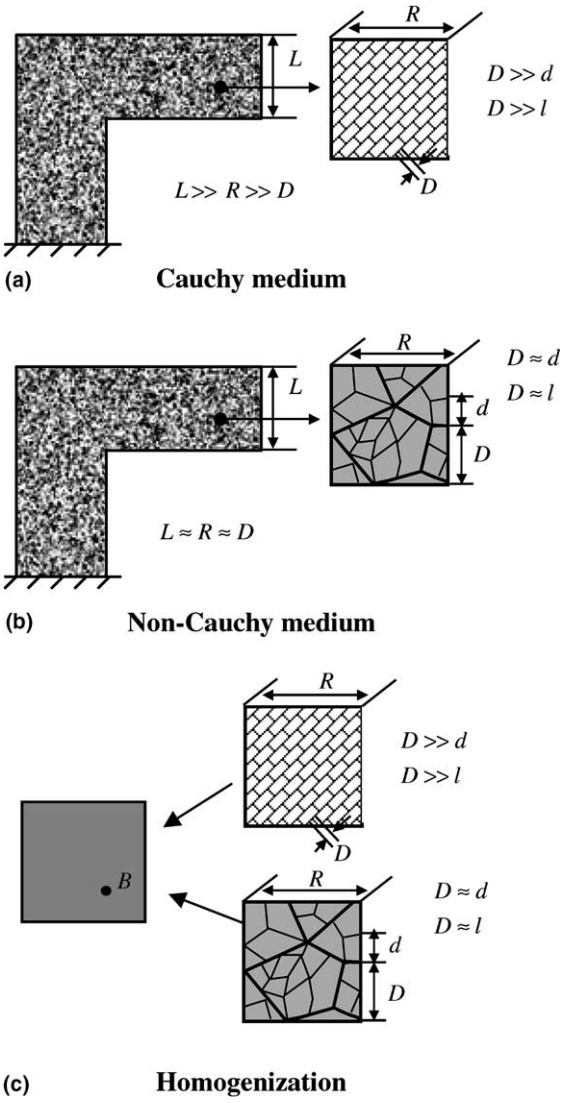


Fig. 2. Length scale conditions in crystalline solids: (a) Cauchy medium; (b) higher-order medium; (c) homogenization model.

and illustrated schematically in Fig. 2, for homogeneous materials, classical continuum mechanics applies when $L \gg R \gg D \gg d$ and $L \gg R \gg D \gg l$ and, correspondingly, the materials are called the Cauchy medium (Fig. 2a); higher-order continuum mechanics theories prevail if $L \approx R \approx D \approx d \approx l \sim 1$ μm, with the materials referred to as the non-Cauchy or higher-order continuum (Fig. 2b). Another length scale, $b \sim 0.01$ μm, representing the average spacing of dislocations, has been neglected hitherto by both classical and higher-order phenomenological plasticity theories. A higher-order continuum theory with atomic basis and using the dislocation spacing $b$ as the relevant length scale has been put forward recently by Garkipati (2003). In the present investigation, the assumption that $l \gg b$ will be retained.

For both the Cauchy medium (Fig. 2a) and the higher-order medium (Fig. 2b), the homogenization model is shown in Fig. 2c. In the homogenized medium, it is assumed that the microstructural details of a material point $B$ can be neglected. The difference between the two different types of medium is that, after homogenization, the deformation of a higher-order continuum needs to be described, in addition to the classical Cauchy stresses and strains, by introducing higher-order stress/strain measures and the associated material length scales, whereas the latter are not needed for a Cauchy medium.

If the length parameters $L$, $R$, $D$ and/or $d$ are all on the order of $1 \sim 100$ nm, recent experimental evidence suggests that the existing higher-order continuum theories may no longer be valid (Haque and Saif, 2003). Using a novel testing technique based on MEMS (microelectro-mechanical systems), Haque and Saif (2002, 2003) found that for thin aluminum films with thickness less than 100 nm and grain sizes smaller than 50 nm, it is energetically unfavorable for the grains to accommodate dislocations (Wang et al., 1995), and hence the dislocation mechanism and the associated plasticity strain gradient effect cannot be used to explain the remarkable strengthening and (yielding) of the nanoscale thin film both under uniaxial tension and bending. In comparison, no such size dependence is observed during the uniaxial tension of a pure copper wire with diameter ranging from 12 to 170 μm (Fleck et al., 1994). Furthermore, under TEM (tunneling electronic microscope), Haque and Saif (2003) observed extensive dislocation activities (with ~5 nm dislocation spacing) in 200 nm thick films, but no evidence of dislocations is found for 100 nm specimens (which nonetheless still exhibit pronounced yielding behavior).

### 1.2. Length scales and size effects in particulate composites

The classcal micromechanics for a particle-reinforced matrix composite assumes that both the reinforcements and the matrix are homogenized Cauchy media: the homogenized equivalent material of the composite itself is also a Cauchy medium, with $L \gg R \gg D$ (Zaoui, 2002). Here, the microstructural details of the matrix, e.g., constituents, voids and precipitates of size $d$ and strain gradient features, are ignored, with the assumption that $D \gg d$ and $D \gg l$. In other words, the classical micromechanics is valid if $L \gg R \gg D \gg d$ and $L \gg R \gg D \gg l$ (Fig. 3a).

However, for metal matrix composites, if the plasticity length scale $l$ and/or the constituent size $d$ of the matrix have the same order of magnitude as that of the particle reinforcements, i.e., $D \approx d$ and $D \approx l$ (Fig. 3a,b), the non-local nature of the matrix material must be taken into account. In particular, a higher-order theory of plasticity for the matrix needs to be employed when $D \approx l \sim 1$ μm.

For composites having either a Cauchy matrix (Fig. 3a) or a higher-order matrix (Fig. 3b), the continuum model after homogenization is shown in Fig. 3c. Comments made previously regarding Fig. 2c for a crystalline solid still apply here for the homogenized matrix containing particulate reinforcements.

Micromechanical methods for the length scale condition $L \gg R \gg D$ ($\gg d \gg b$) and $L \gg R \gg D$ ($\gg l \gg b$) have been well developed in the past

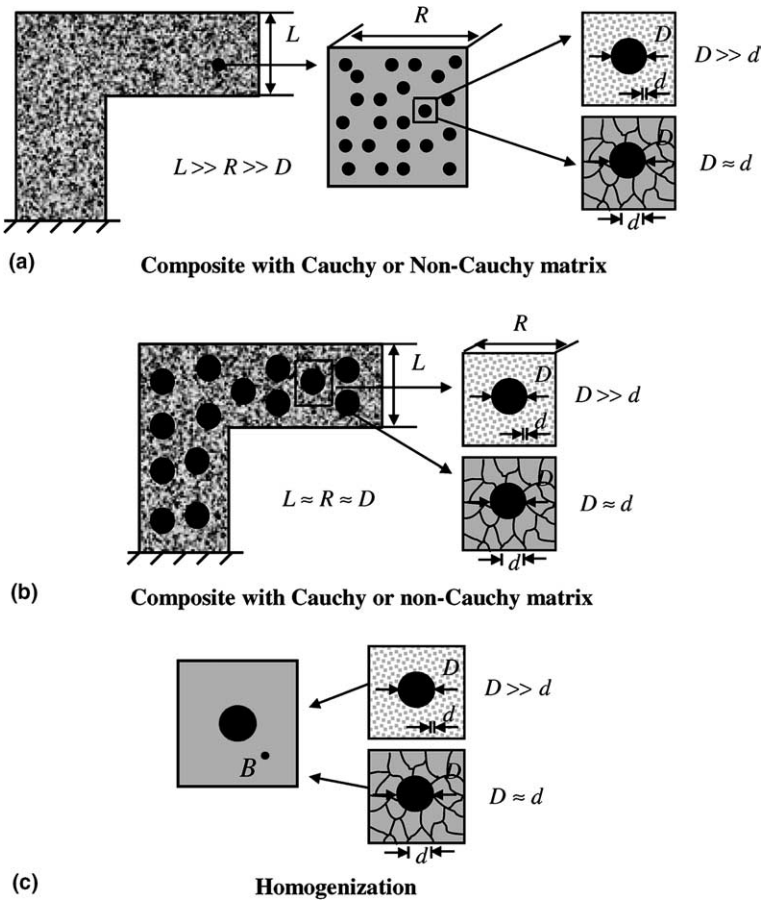


Fig. 3. Length scale conditions in particulate composites: (a) Cauchy medium; (b) higher-order medium; (c) homogenization model.

decades, wherein the local material and the corresponding homogenized material can be both modeled as the Cauchy medium. The bounding methods proposed by Hashin and Shtrikman (1963) and Milton (1981) have proven to be of enduring allure for a wide range of applications, see, e.g., Torquato (1991, 2002) for a comprehensive review. Other approximate methods have also been widely used to predict the overall thermomechanical properties of various composites with particular microstructures, such as the Mori–Tanaka model (Mori and Tanaka, 1973), the double-inclusion model (Hori and Nemat-Nasser, 1993), the self-consistent method (Kroner, 1958), and the generalized self-consistent method (see, e.g., Christensen and Lo, 1979). The interconnections amongst these approximate methods can be found in Hu and Weng (2000a,b).

To predict the non-linear effective behavior of a composite material, linearized methods such as the secant moduli method and its modification (Tandon and Weng, 1988; Qiu and Weng, 1992; Hu, 1996), the variational method (Ponte Castañeda, 1991), and the semi-analytical unit cell model (Ji and Wang, 2003) have been proposed. Although these methods provide useful tools to bridge the macroscopic properties of the composite with its microstructural parameters, they all fail to predict the dependence of its overall plastic behavior on reinforcement size at the micron scale.

To include the size dependence of the overall property for a non-linear composite, two strategies may be adopted. The first stems from the viewpoint of materials science by introducing the geometrically necessary dislocation hardening or dislocation interaction (see, e.g., Fleck et al., 1994; Yashin et al., 2001), whereas the second originates from the viewpoint of continuum mechanics by introducing higher-order continuum theories (see, e.g., Smyshlyaev and Fleck, 1994; Wei, 2001; Tsagrakis and Aifantis, 2002; Forest et al., 2000; Chen and Wang, 2002; Liu and Hu, in press). The latter approach will be exploited in this study.

### 1.3. Scope and objectives

With focus placed on isotropic particle-reinforced metal matrix composites, this paper aims to explore the interconnections between material length scales and geometric sizes (and/or material constants), to develop a higher-order continuum theory for non-linear non-Cauchy media, to extend the variational principle of Ponte Castañeda (1991) for a non-linear Cauchy composite to a non-linear non-Cauchy composite, and to predict analytically the overall mechanical response (yielding/strengthening and strain hardening) of the non-linear composite. Here, the size scales considered are such that $L \gg R \gg D \approx l \sim 1$ μm. Under these conditions, as in homogeneous crystalline solids (but under the conditions that $L \approx R \approx D \approx l \sim 1$ μm), similarly compelling evidence of strong size dependence of yielding/strengthening exists in particle/fiber-reinforced metal matrix composites (see, e.g., Smyshlyaev and Fleck, 1994, 1995; Lloyd, 1994; Kouzeli and Mortensen, 2002; Fig. 1). For simplicity, our analytical study will be restricted to small strain/small rotation time-independent non-linearity and, further, to isotropic composites with particles firmly bonded to the metal matrix (whose microstructural details are ignored, i.e., the size parameter $d$ is absent). The volume fraction and size of the particles are taken into account, but not the particle shape and distribution. [2]

In this paper, the variational method of Ponte Castañeda (1991) and the deformation theory of micropolar plasticity are used in order to obtain simple closed form solutions. We note, on one hand, numerical schemes such as the method of finite elements (Forest et al., 2000; Bassani et al., 2001; Xue et al., 2002) have been applied to non-local composites, but not all numerical methods are suitable or can give satisfactory predictions (Fleck and Hutchinson, 2001). For example, different types of higher-order finite element may yield rather different solutions for the same problem (Shi et al., 2000), and it is cumbersome to implement non-standard boundary and interface conditions numerically. On the other hand, for proportional or nearly proportional loading, the

[2] For a given phase distribution and a fixed volume ratio, Xue et al. (2002) found that the difference between the size effects induced separately by spherical and cylindrical particles is small.

deformation theory can provide analytical solutions for basic problems, is much simpler to implement numerically, and its validity and applicability has been well addressed (see, e.g., Budiansky, 1959; Fleck and Hutchinson, 2001).

## 2. Micropolar elasticity and plasticity: fundamental formulations

### 2.1. Micropolar elasticity

Following Koiter (1964) and Eringen (1968), to extend the classical Cauchy continuum mechanics theory to a higher-order medium, it is assumed that any material point is endowed with an internal microstructure. Accordingly, three displacements $u_i$ ($i=1, 2, 3$) are employed in the usual way to characterize the macroscopic motion of the material point, and three additional microrotation angles (or angular displacements) $\phi_i$ ($i=1, 2, 3$) are introduced to describe the rotation of the microstructure within the material point. Furthermore, it is assumed that the rotation field is kinematically independent from the displacement field, and $\phi_i$ is distinct from the material rotation $\theta_i \equiv (1/2)e_{ijk}u_{k,j}$, where $e_{ijk}$ is the permutation tensor, repeated indices imply summation over (1, 2, 3), the subscript preceded by a comma denotes the derivative with respect to the corresponding spatial coordinate, and the Cartesian system $(x_1, x_2, x_3)$ is adopted throughout the paper. The corresponding continuum theory is called the micropolar theory, being different from other higher-order continuum theories such as the micromorphic theory (Eringen, 1999), the microstretch theory (Markov, 1981), and the strain gradient theory (German, 1973). More detailed discussions on the micropolar elasticity theory can be found in the monographs by Eringen (1999) and by Nowacki (1986). Jasiuk and Ostoja-Starzewski (1995) applied the micropolar elasticity theory to analyze the materials with holes and intrusions, whilst Lubarda and Markenscoff (2000, 2003) discussed the conservation integrals in couple stress and micropolar elasticity.

With micropolar continuum theory, not only forces but also moments can be transmitted across the surface of a material element. Similar to the conventional strain tensor $\varepsilon_{ij}$ (defined as the gradient of the displacement vector) which is the work conjugate of the Cauchy stress tensor $\sigma_{ij}$, the gradient of the rotation vector is defined as the torsion (or curvature) tensor $k_{ij}$, which is related by a constitutive relation to the couple stress tensor $m_{ij}$. Both the newly introduced couple stress (torsion) tensor and the classical stress (strain) tensor are in general non-symmetric. With body forces and body couples neglected, a well-posed micropolar boundary value problem for a continuum solid of volume $V$ and bounded by surface $S$ can be established by the following three sets of governing equations:

$$\begin{cases} \varepsilon_{ij} = u_{j,i} - e_{kij}\phi_k \\ k_{ij} = \phi_{j,i} \end{cases} \quad \text{(Kinematic relations)}, \tag{2.1}$$

$$\begin{cases} \sigma_{ij,i} = 0 \\ m_{ij,i} + e_{jik}\sigma_{ik} = 0 \end{cases} \quad \text{(Equilibrium equations)}, \tag{2.2}$$

$$\begin{cases} \sigma_{ij} = C_{ijkl}\varepsilon_{kl} + B_{ijkl}k_{kl} \\ m_{ij} = B_{ijkl}\varepsilon_{kl} + D_{ijkl}k_{kl} \end{cases} \quad \text{(Constitutive laws)}, \tag{2.3}$$

and the corresponding boundary conditions:

$$\sigma_{ij}n_i = p_j, \quad m_{ij}n_i = z_j, \quad \text{on } \Gamma^\sigma, \tag{2.4}$$

$$u_i = u_i^b, \quad \phi_i = \phi_i^b, \quad \text{on } \Gamma^u, \tag{2.5}$$

where $B_{ijkl}$, $C_{ijkl}$ and $D_{ijkl}$ are the elastic constant tensors, $p_j$ and $z_j$ are the surface force and moment vectors acting on a surface element with unit normal $n_i$, $\Gamma^\sigma$ is part of the free surface $S$ where tractions and moments are prescribed, and $\Gamma^u = S - \Gamma^\sigma$ is the remaining part of the surface where displacements $u_i^b$ and $\phi_i^b$ are specified.

The preceding governing equations can be obtained from the principle of minimum potential energy and the principle of minimum complementary energy (see, e.g., Koiter, 1964; Fleck and Hutchinson, 1993). Let $(u_i^c, \phi_i^c)$ represent any set of kinematically admissible displacement fields that satisfy the compatibility condition (2.1) and

kinematic boundary condition (2.5), and let $(\sigma^*_{ij}, m^*_{ij})$ denote an arbitrary set of statically admissible stress fields that satisfy the equilibrium condition (2.2) and force boundary condition (2.4). Let $(u_i, \phi_i)$ and $(\sigma_{ij}, m_{ij})$ be the actual solutions of the problem. For all kinematically admissible displacement fields $(u^c_i, \phi^c_i)$ and all statically admissible stress fields $(\sigma^*_{ij}, m^*_{ij})$, the principle of minimum potential energy and the principle of minimum complementary energy dictate (see, e.g., Nowacki, 1986):

$$\begin{aligned} -W(\boldsymbol{\sigma}^*, \mathbf{m}^*) &\leqslant -W(\boldsymbol{\sigma}, \mathbf{m}) \\ &= U(\mathbf{u}, \boldsymbol{\phi}) \leqslant U(\mathbf{u}^c, \boldsymbol{\phi}^c), \end{aligned} \tag{2.6}$$

where $W(\boldsymbol{\sigma}^*, \mathbf{m}^*)$ and $U(\mathbf{u}^c, \boldsymbol{\phi}^c)$ are separately the complementary energy and potential energy of the system, defined by:

$$\begin{aligned} W(\boldsymbol{\sigma}^*, \mathbf{m}^*) &= \int_V w(\boldsymbol{\sigma}^*, \mathbf{m}^*) \mathrm{d}V \\ &\quad - \int_{\Gamma^u} (\mathbf{p}^* \mathbf{u}^b + \mathbf{m}^* \boldsymbol{\phi}^b) \mathrm{d}S, \end{aligned} \tag{2.7a}$$

$$\begin{aligned} U(\mathbf{u}^c, \boldsymbol{\phi}^c) &= \int_V u(\mathbf{u}^c, \boldsymbol{\phi}^c) \mathrm{d}V \\ &\quad - \int_{\Gamma^\sigma} (\mathbf{p}^b \mathbf{u}^c + \mathbf{m}^b \boldsymbol{\phi}^c) \mathrm{d}S. \end{aligned} \tag{2.7b}$$

In the above equations, $w(\boldsymbol{\sigma}^*, \mathbf{m}^*)$ and $u(\mathbf{u}^c, \boldsymbol{\phi}^c)$ are the strain and stress potentials, respectively, and boldfaced symbols represent vectors or matrices. The actual displacement and stress fields minimize the complementary energy and the potential energy, as expressed mathematically by (2.6). Correspondingly, the principle of virtual work for a micropolar solid can be written as:

$$\int_V [\sigma_{ij} \delta \varepsilon_{ij} + m_{ij} \delta k_{ij}] \mathrm{d}V = \int_S (p_i \delta u_i + z_i \delta \phi_i) \mathrm{d}S. \tag{2.8}$$

The study below will be restricted to isotropic micropolar continuum with centro-symmetry (Eringen, 1999; Nowacki, 1986), namely

$$B_{ijkl} = 0, \tag{2.9a}$$

$$C_{ijkl} = \lambda \delta_{ij} \delta_{kl} + (\mu + \kappa) \delta_{jk} \delta_{il} + (\mu - \kappa) \delta_{ik} \delta_{jl}, \tag{2.9b}$$

$$D_{ijkl} = \alpha \delta_{ij} \delta_{kl} + (\beta + \gamma) \delta_{jk} \delta_{il} + (\beta - \gamma) \delta_{ik} \delta_{jl}, \tag{2.9c}$$

where $(\mu, \lambda)$ are the classical Lame constants, $(\kappa, \gamma, \beta, \alpha)$ are new material constants introduced in micropolar theory, and $\delta_{ij}$ is the Kronecker delta.

With $\sigma'_{(ij)}$, $\sigma_{\langle ij \rangle}$, $\sigma$ $(\equiv \sigma_{ii})$ and $\varepsilon'_{(ij)}$, $\varepsilon_{\langle ij \rangle}$, $\varepsilon$ $(\equiv \varepsilon_{ii})$ denoting separately the deviatoric symmetric, anti-symmetric and hydrostatic parts of the stress and strain tensors, and similar notations for the couple-stress and torsion tensors, the well-established elastic constitutive relations for a linear isotropic micropolar material can be rewritten as (Nowacki, 1986):

$$\sigma'_{(ij)} = 2\mu \varepsilon'_{(ij)}, \quad \sigma_{\langle ij \rangle} = 2\kappa \varepsilon_{\langle ij \rangle}, \quad \sigma = 3K\varepsilon, \tag{2.10a}$$

$$m'_{(ij)} = 2\beta k'_{(ij)}, \quad m_{\langle ij \rangle} = 2\gamma k_{\langle ij \rangle}, \quad m = 3Nk, \tag{2.10b}$$

and

$$K = \lambda + \frac{2}{3}\mu, \quad N = \alpha + \frac{2}{3}\beta, \tag{2.11}$$

where $K$ is the bulk modulus, $N$ can be regarded as the corresponding stiffness measure for torsion, and symbols $(\ )$ and $\langle\ \rangle$ in the subscript denote the symmetric and anti-symmetric parts of a tensor, respectively. The strain energy density for such a micropolar continuum then becomes:

$$\begin{aligned} w &= \frac{1}{4\mu} \sigma'_{(ij)} \sigma'_{(ij)} + \frac{1}{4\kappa} \sigma_{\langle ij \rangle} \sigma_{\langle ij \rangle} + \frac{1}{18K} \sigma^2 \\ &\quad + \frac{1}{4\beta} m'_{(ij)} m'_{(ij)} + \frac{1}{4\gamma} m_{\langle ij \rangle} m_{\langle ij \rangle} + \frac{1}{18N} m^2, \end{aligned} \tag{2.12}$$

from which the constitutive laws can be obtained as:

$$\varepsilon'_{(ij)} = \frac{\partial w}{\partial \sigma'_{(ij)}}, \quad \varepsilon_{\langle ij \rangle} = \frac{\partial w}{\partial \sigma_{\langle ij \rangle}}, \quad \varepsilon = \frac{1}{3} \frac{\partial w}{\partial \sigma}, \tag{2.13a}$$

$$k'_{(ij)} = \frac{\partial w}{\partial m'_{(ij)}}, \quad k_{\langle ij \rangle} = \frac{\partial w}{\partial m_{\langle ij \rangle}}, \quad k = \frac{1}{3} \frac{\partial w}{\partial m}. \tag{2.13b}$$

There are two distinct sets of moduli: $(\mu,\lambda,\kappa)$ which relate the traditional stresses and strains and have a dimension of force per unit area, and $(\gamma,\beta,\alpha)$ which relate the higher-order couple-stresses and torsions, with a dimension of force. Due to the dimensional difference between the two sets of moduli, at least three intrinsic characteristic lengths can be defined for an isotropic elastic micropolar material. These elasticity length parameters can be defined in different ways; in this paper, they are defined as:

$$l_1=(\gamma/\mu)^{1/2},\quad l_2=(\beta/\mu)^{1/2},\quad l_3=(\alpha/\mu)^{1/2}. \tag{2.14}$$

### 2.2. Micropolar plasticity

The plasticity theory for a micopolar material is not as well developed as the micropolar elasticity. A deformation version of the phenomenological theory of micropolar plasticity is presented below, which is analogous to that of Chen and Wang (2001) proposed from a different perspective. It should be emphasized that the micropolar theory used in this paper is different from the strain gradient theory proposed by Fleck and Hutchinson (1993) for metals and Smyshlyaev and Fleck (1994, 1995) for non-linear composites, since microrotation is independent of displacement gradient in the micropolar theory but not in the strain gradient theory.

For a non-linear micropolar material, let the generalized equivalent stress be defined as (Lippmann, 1995; Fleck and Hutchinson, 2001; Chen and Wang, 2001; Liu and Hu, in press):

$$\overline{\sigma}_{\mathrm{e}}^2=\sigma_{\mathrm{e}}^2+\bar{l}_1^{-2}m_{\langle\mathrm{e}\rangle}^2+\bar{l}_2^{-2}m_{\langle\mathrm{e}\rangle}^2, \tag{2.15}$$

where $(\bar{l}_1,\bar{l}_2)$ are material length parameters appearing on dimensional grounds, and

$$\sigma_{\mathrm{e}}\equiv\sigma_{\langle\mathrm{e}\rangle}=\sqrt{\frac{3}{2}\sigma'_{\langle ij\rangle}\sigma'_{\langle ij\rangle}},$$
$$m_{\langle\mathrm{e}\rangle}=\sqrt{\frac{3}{2}m'_{\langle ij\rangle}m'_{\langle ij\rangle}},\quad m_{\langle\mathrm{e}\rangle}=\sqrt{\frac{3}{2}m_{\langle ij\rangle}m_{\langle ij\rangle}}, \tag{2.16}$$

are the usual von Mises effective stress and the analogous effective couple stresses, respectively.

Let the generalized yield surface be specified by:

$$\Phi(\overline{\sigma}_{\mathrm{e}},\sigma_{\mathrm{y}})=\overline{\sigma}_{\mathrm{e}}-\sigma_{\mathrm{y}}=0, \tag{2.17}$$

where $\sigma_{\mathrm{y}}$ is the current uniaxial flow stress. When the non-linear micropolar material is subjected to a uniaxial tensile stress $\sigma_{11}$, $\bar{\sigma}_{\mathrm{e}}=\sigma_{11}$, and yielding occurs when $\sigma_{11}=\sigma_{\mathrm{y}}$. In the absence of plastic flow or micropolar effect, $\overline{\sigma}_{\mathrm{e}}=\sigma_{\mathrm{e}}$. Also note that $(\bar{l}_1,\bar{l}_2)$ may in the main be interpreted as the characteristic plasticity length scales. Following Fleck and Hutchinson (1994) Fleck and Hutchinson (1993) and Chen and Wang (2001), the stress potential for a non-linear micropolar material may be written as:

$$w=w_0(\overline{\sigma}_{\mathrm{e}})+\frac{1}{6\kappa}\sigma_{\langle\mathrm{e}\rangle}^2+\frac{1}{18K}\sigma^2+\frac{1}{18N}m^2 \tag{2.18a}$$

or, equivalently,

$$w=w_0(\overline{\sigma}_{\mathrm{e}})+\frac{1}{6\mu}\left[\frac{\sigma_{\langle\mathrm{e}\rangle}^2}{\kappa/\mu}+\frac{\sigma^2}{2+3\lambda/\mu}+\frac{m^2}{2l_2^2+3l_3^2}\right]. \tag{2.18b}$$

Here, $\sigma_{\langle\mathrm{e}\rangle}=\sqrt{\frac{3}{2}\sigma_{\langle ij\rangle}\sigma_{\langle ij\rangle}}$, and $w_0(\overline{\sigma}_{\mathrm{e}})$ is specified by a power law relation as:

$$w_0(\overline{\sigma}_{\mathrm{e}})=\frac{\overline{\sigma}_{\mathrm{e}}^2}{6\mu}+\frac{n}{n+1}\frac{1}{H^{1/n}}(\overline{\sigma}_{\mathrm{e}}-\sigma_{\mathrm{y}})^{\frac{n+1}{n}}, \tag{2.19}$$

where $n$ is the strain hardening exponent and $H$ is the hardening modulus. In the absence of plasticity effects, (2.19) reduces to the elastic counterpart (2.12).

In the linear elastic range (i.e., $\overline{\sigma}_{\mathrm{e}}<\sigma_{\mathrm{y}}$), substitution of (2.19) into (2.13) leads to the same stress (couple stress) and strain (torsion) relations as those shown in (2.10). In the elastic–plastic regime, an identical manipulation leads to:

$$\varepsilon'_{\langle ij\rangle}=\frac{1}{2\mu^{\mathrm{s}}}\frac{\sigma'_{\langle ij\rangle}}{\overline{\sigma}_{\mathrm{e}}},\quad \varepsilon_{\langle ij\rangle}=\frac{1}{2\kappa^{\mathrm{s}}}\sigma_{\langle ij\rangle},\quad \varepsilon=\frac{1}{3K^{\mathrm{s}}}\sigma, \tag{2.20a}$$

$$k'_{\langle ij\rangle}=\frac{1}{2\beta^{\mathrm{s}}}\frac{m'_{\langle ij\rangle}}{\overline{\sigma}_{\mathrm{e}}},\quad k'_{\langle ij\rangle}=\frac{1}{2\gamma^{\mathrm{s}}}\frac{m'_{\langle ij\rangle}}{\overline{\sigma}_{\mathrm{e}}},\quad k=\frac{1}{3N^{\mathrm{s}}}m, \tag{2.20b}$$

where

$$\mu^{\mathrm{s}}=\frac{1}{(1/\mu)+3[(\bar{\sigma}_{\mathrm{e}}-\sigma_{\mathrm{y}})/H]^{1/n}/\bar{\sigma}_{\mathrm{e}}},$$
$$\kappa^{\mathrm{s}}=\kappa,\quad K^{\mathrm{s}}=K, \tag{2.21a}$$

$$\beta^{s} = \overline{l}_1^2 \mu^{s}, \quad \gamma^{s} = \overline{l}_2^2 \mu^{s}, \quad N^{s} = N, \tag{2.21b}$$

and the superscript 's' is used to denote the secant moduli of the non-linear micropolar material (Liu and Hu, in press). These secant moduli will be used in the following sections to determine the non-linear effective properties of a particle-reinforced micropolar composite.

It is seen from (2.21b) that, to have a smooth transition from elasticity to plasticity, $\overline{l}_1 = l_1$ and $l_2 = l_2$ are required, i.e., there is no difference between elastic and plastic length scales. Consequently, for simplicity, $l_1 = l_2 = l_3 = \overline{l}_1 = \overline{l}_2 \equiv l_m$ will be assumed in the present study so that only one length scale appears in the theory.

## 3. Variational method for non-linear micropolar composites

### 3.1. Micro–macro transition principle for heterogeneous micropolar medium

As previously discussed, this study will focus on the length scale condition $L \gg R \gg D \approx d$ (Fig. 3a) for particle-reinforced micropolar composites. That is, the particle size $D$ is sufficiently small in comparison with the RVE size $R$, and the effect of macroscopic stress gradient on the RVE can be neglected (i.e., $R$ is sufficiently small in comparison with the structural dimension $L$). In other words, whilst the effective medium can be considered as the classical Cauchy medium, the local constituents are idealized as micropolar materials due to the coarse microstructure of the matrix ($D \approx d$). Consequently, the following traditional boundary conditions can be applied:

$$\sigma_{ij} n_i = \Sigma_{(ij)} n_i, \quad m_{ij} n_i = 0, \tag{3.1}$$

where $\langle \sigma_{(ij)} \rangle = \Sigma_{(ij)} \equiv \Sigma_{ij}^{\mathrm{sym}}$. Here, $\langle \bullet \rangle$ represents the volume average of the said quantity over the RVE, and the average stress $\Sigma_{(ij)}$ is symmetric and constant over the RVE. In the case of elasticity, it has been demonstrated that the following micro–macro transition principle holds (Xun et al., 2004; Liu and Hu, in press):

$$\langle \boldsymbol{\sigma}\boldsymbol{\varepsilon} + \mathbf{m}\mathbf{k} \rangle = \boldsymbol{\Sigma}^{\mathrm{sym}} \overline{\mathbf{M}}^{\mathrm{sym}} \boldsymbol{\Sigma}^{\mathrm{sym}}, \tag{3.2}$$

where the overbar is used to denote the effective quantities of the composite, and $\overline{\mathbf{M}}^{\mathrm{sym}}$ is the effective compliance tensor of the composite that relates the average symmetric stress and strain of the RVE as $\boldsymbol{\Sigma}^{\mathrm{sym}} = \overline{\mathbf{M}}^{\mathrm{sym}} \langle \boldsymbol{\varepsilon}^{\mathrm{sym}} \rangle$.

For non-linear elasticity, the local strain potential is defined by Eqs. (2.18) and (2.19). The corresponding effective macroscopic potential of the micropolar composite is defined in the same way as that in classical micromechanics:

$$\overline{W}_{\mathrm{eff}}(\boldsymbol{\Sigma}^{\mathrm{sym}}) = \inf_{\forall(\boldsymbol{\sigma}^*, \mathbf{m}^*) \in SA} \langle w(\boldsymbol{\sigma}^*, \mathbf{m}^*; \mathbf{x}) \rangle, \tag{3.3}$$

where SA represents the set of all statistically admissible fields that satisfy the boundary condition (3.1) and the equilibrium condition (2.2), and the operator Inf means the minimum.

The same process as that shown above for the force boundary condition (3.1) holds for the following displacement boundary condition, $\varepsilon_{ij} x_i = E_{(ij)} x_i$ and $\phi_i = 0$ where $E_{(ij)} \equiv E_{ij}^{\mathrm{sym}} = \langle \varepsilon_{(ij)} \rangle$ is the symmetric part of the average strain, which allows one to define the effective stiffness tensor of the micropolar composite for linear elasticity and the stress potential for non-linear elasticity.

### 3.2. Variational method for non-linear micropolar composites

We will now apply the variational principle to the RVE of a non-linear micropolar composite under the boundary condition of (3.1). It is assumed that the non-linear composite contains $N$ phases and, for phase $r$ (of volume fraction $c_r$), its strain potential $w_r$ is defined by (2.19). Following Ponte Castañeda (1991), we introduce a linear comparison material associated with phase $r$ and write its strain potential as:

$$w_r^{s}(\boldsymbol{\sigma}, \mathbf{m}) = \frac{1}{2} \boldsymbol{\sigma} \mathbf{M}_r^{s} \boldsymbol{\sigma} + \frac{1}{2} \mathbf{m} \mathbf{H}_r^{s} \mathbf{m}, \tag{3.4a}$$

where the superscript 's' represents quantities associated with the non-Cauchy matrix of the linear comparison micropolar composite, and $\mathbf{M}_r^{s}$ and $\mathbf{H}_r^{s}$ are the local compliance tensors of phase $r$ in the linear comparison composite. Let

$$V^{r}(\mathbf{M}_r^{s}, \mathbf{H}_r^{s}) = \sup_{\forall(\boldsymbol{\sigma}, \mathbf{m})} [w_r^{s}(\boldsymbol{\sigma}, \mathbf{m}) - w_r(\boldsymbol{\sigma}, \mathbf{m})], \tag{3.4b}$$

where the operator Sup means the supreme operation.

It will now be shown that the linear comparison material as defined above has a secant compliance of the actual material. Multiplying both sides of (3.4) by the characteristic function $\chi_r(\boldsymbol{x})$ of phase $r$ ($\chi_r=1$ for all points inside the phase; otherwise $\chi_r=0$; $r=1,2,\ldots,N$), one can rearrange (3.4) for the whole composite, as:

$$w(\boldsymbol{\sigma},\mathbf{m};\mathbf{x}) \geqslant w^{s}(\boldsymbol{\sigma},\mathbf{m};\mathbf{x}) - V(\mathbf{M}^{s},\mathbf{H}^{s};\mathbf{x}). \tag{3.5}$$

Averaging both sides of (3.5) over the RVE and then carrying out the minimization over all the statistically admissible fields $(\boldsymbol{\sigma},\mathbf{m})$—noting that the statistically admissible fields for the non-linear composite are automatically the statistically admissible fields for the linear comparison composite under the same loading condition—we arrive at:

$$\overline{W}_{\text{eff}} \geqslant \overline{W}^{s}(\mathbf{M}^{s},\mathbf{H}^{s};\boldsymbol{\Sigma}^{\text{sym}}) - \overline{V}(\mathbf{M}^{s},\mathbf{H}^{s}), \tag{3.6}$$

where $\overline{W}^{s}(\mathbf{M}^{s},\boldsymbol{H}^{s};\boldsymbol{\Sigma}^{\text{sym}})$ is the effective macroscopic strain potential for the linear comparison composite with local compliance tensors $(\mathbf{M}^{s}_{r},\mathbf{H}^{s}_{r})$ for phase $r$, and

$$\overline{V}(\mathbf{M}^{s},\mathbf{H}^{s}) = \sum_{r=1}^{N} c_r V_r(\mathbf{M}^{s}_{r},\mathbf{H}^{s}_{r}). \tag{3.7}$$

The same as Ponte Castañeda's variational method for a non-linear Cauchy composite, the bounds and estimate of the effective strain potential for a non-linear micropolar composite can be obtained by the corresponding bounds and estimate for the corresponding linear comparison micropolar composite. These bounds and estimate can be optimized over all the possible linear comparison composites, as:

$$\begin{aligned}\overline{W}_{\text{eff}} \geqslant \overline{W}_{\text{eff}} &\equiv \operatorname*{Sup}_{\forall(\mathbf{M}^{s},\mathbf{H}^{s})} [\overline{W}^{s}(\mathbf{M}^{s},\mathbf{H}^{s};\boldsymbol{\Sigma}^{\text{sym}}) - \overline{V}(\mathbf{M}^{s},\mathbf{H}^{s})] \\ &\equiv \operatorname*{Sup}_{\forall(\mathbf{M}^{s},\mathbf{H}^{s})} [F],\end{aligned} \tag{3.8}$$

which represents the micropolar version of Ponte Castañeda's variational method for non-linear micropolar composites.

### 3.3. Interpretation as the secant moduli method

For a Cauchy medium, Qiu and Weng (1992), Suquet (1995) and Hu (1996) have demonstrated that the variational method of Ponte Castañeda (1991) can be interpreted as the secant moduli method based on the second-order stress moments. We will demonstrate next that the micropolar version of Ponte Castañeda's variational method can be exactly interpreted as the secant moduli method based on the second-order stress and couple stress moments, proposed recently by Liu and Hu (in press).

Firstly, by evaluating the supreme operation in Eq. (3.4), we obtain:

$$\mathbf{M}^{s}_{r}\boldsymbol{\sigma} = \frac{\partial w_r}{\partial \boldsymbol{\sigma}}, \quad \mathbf{H}^{s}_{r}\mathbf{m} = \frac{\partial w_r}{\partial \mathbf{m}}. \tag{3.9}$$

Eq. (3.9) indicates that the compliance of phase $r$ in the linear comparison micropolar material is always equal to the secant compliance tensor of phase $r$ in the actual micropolar material. Next, the supreme operation in (3.8) that determines the evolution of local secant compliance tensors as a function of external load is carried out, yielding:

$$\begin{aligned}&\langle \chi_r \boldsymbol{\sigma}_r \otimes \boldsymbol{\sigma}_r\rangle + 2\left\langle \chi_r \boldsymbol{\sigma}_r \mathbf{M}^{s}_{r} \frac{\partial \boldsymbol{\sigma}_r}{\partial \mathbf{M}^{s}_{r}}\right\rangle - 2\left\langle \chi_r \frac{\partial w_r}{\partial \boldsymbol{\sigma}_r}\frac{\partial \boldsymbol{\sigma}_r}{\partial \mathbf{M}^{s}_{r}}\right\rangle \\ &\quad = \boldsymbol{\Sigma}^{\text{sym}} \frac{\partial \overline{\mathbf{M}}^{\text{sym}}}{\partial \mathbf{M}^{s}_{r}} \boldsymbol{\Sigma}^{\text{sym}},\end{aligned} \tag{3.10a}$$

$$\begin{aligned}&\langle \chi_r \mathbf{m}_r \otimes \mathbf{m}_r\rangle + 2\left\langle \chi_r \mathbf{m}_r \mathbf{H}^{s}_{r} \frac{\partial \mathbf{m}_r}{\partial \mathbf{H}^{s}_{r}}\right\rangle - 2\left\langle \chi_r \frac{\partial w_r}{\partial \mathbf{m}_r}\frac{\partial \mathbf{m}_r}{\partial \mathbf{H}^{s}_{r}}\right\rangle \\ &\quad = \boldsymbol{\Sigma}^{\text{sym}} \frac{\partial \overline{\mathbf{M}}^{\text{sym}}}{\partial \mathbf{H}^{s}_{r}} \boldsymbol{\Sigma}^{\text{sym}},\end{aligned} \tag{3.10b}$$

where $\overline{\mathbf{M}}^{\text{sym}}$ is the effective compliance tensor of the linear comparison micropolar composite, and $\otimes$ denotes the dydic operation. In deriving (3.10a,b), the following properties of a centro-symmetric material have been utilized:

$$\frac{\partial \mathbf{m}_r}{\partial \mathbf{M}^{s}_{r}} = 0, \quad \frac{\partial \boldsymbol{\sigma}_r}{\partial \mathbf{H}^{s}_{r}} = 0. \tag{3.11}$$

With the help of (3.9), Eqs. (3.10a,b) can be further reduced to:

$$c_r\langle \boldsymbol{\sigma}_r \otimes \boldsymbol{\sigma}_r\rangle_r = \boldsymbol{\Sigma}^{\text{sym}} \frac{\partial \overline{\mathbf{M}}^{\text{sym}}}{\partial \mathbf{M}^{s}_{r}} \boldsymbol{\Sigma}^{\text{sym}}, \tag{3.12a}$$

$$c_r\langle \mathbf{m}_r \otimes \mathbf{m}_r \rangle_r = \boldsymbol{\Sigma}^{\mathrm{sym}} \frac{\partial \overline{\mathbf{M}}^{\mathrm{sym}}}{\partial \mathbf{H}_r^{\mathrm{s}}} \boldsymbol{\Sigma}^{\mathrm{sym}}, \tag{3.12b}$$

where $\langle \bullet \rangle_r$ means the volume average of the said quantity over phase $r$.

Eqs. (3.11) and (3.12) allow one to evaluate the effective stress defined in (2.15) for the micropolar matrix in the linear comparison composite and, in turn, the evolution of the secant compliance tensor of the matrix in the actual non-linear micropolar composite. The strain and stress relation for the non-linear micropolar composite can be simply obtained as:

$$\begin{aligned} \mathbf{E}^{\mathrm{sym}} &= \frac{\partial \overline{W}_{\mathrm{eff}}}{\partial \boldsymbol{\Sigma}^{\mathrm{sym}}} \\ &= \overline{\mathbf{M}}^{\mathrm{sym}} \boldsymbol{\Sigma}^{\mathrm{sym}} - \frac{\partial F}{\partial \mathbf{M}_r^{\mathrm{s}}} \frac{\partial \mathbf{M}_r^{\mathrm{s}}}{\partial \boldsymbol{\Sigma}^{\mathrm{sym}}} - \frac{\partial F}{\partial \mathbf{H}_r^{\mathrm{s}}} \frac{\partial \mathbf{H}_r^{\mathrm{s}}}{\partial \boldsymbol{\Sigma}^{\mathrm{sym}}}. \end{aligned} \tag{3.13}$$

However, due to the optimization process in (3.8), one has:

$$\frac{\partial F}{\partial \mathbf{M}_r^{\mathrm{s}}} = 0, \quad \frac{\partial F}{\partial \mathbf{H}_r^{\mathrm{s}}} = 0, \tag{3.14}$$

upon which (3.13) reduces to:

$$\mathbf{E}^{\mathrm{sym}} = \overline{\mathbf{M}}^{\mathrm{sym}} \boldsymbol{\Sigma}^{\mathrm{sym}}. \tag{3.15}$$

We have therefore established the equivalence between the effective elastic compliance tensor of the linear comparison micropolar composite and the effective secant compliance tensor of the actual non-linear micropolar composite.

In fact, (3.12a,b) can be derived directly from the fluctuation field method, recently developed by Liu and Hu (in press) for a micropolar composite. From the micro–macro transition principle defined in (3.1), Eq. (3.2) for the linear comparison composite can be rewritten as

$$\langle \boldsymbol{\sigma} \mathbf{M}^{\mathrm{s}} \boldsymbol{\sigma} + \mathbf{m} \mathbf{H}^{\mathrm{s}} \mathbf{m} \rangle = \boldsymbol{\Sigma}^{\mathrm{sym}} \overline{\mathbf{M}}^{\mathrm{sym}} \boldsymbol{\Sigma}^{\mathrm{sym}}. \tag{3.16}$$

With the macroscopic stress $\boldsymbol{\Sigma}^{\mathrm{sym}}$ fixed, the independent variations $\delta \mathbf{M}_r^{\mathrm{s}}$ and $\delta \mathbf{H}_r^{\mathrm{s}}$ of the local compliance tensor for each of the $N$ phases give:

$$\begin{aligned} &c_r\langle \boldsymbol{\sigma} \delta \mathbf{M}_r^{\mathrm{s}} \boldsymbol{\sigma} + \mathbf{m} \delta \mathbf{H}_r^{\mathrm{s}} \mathbf{m} \rangle_r + 2\langle \boldsymbol{\sigma} \mathbf{M}^{\mathrm{s}} \delta \boldsymbol{\sigma} \rangle + 2\langle \mathbf{m} \mathbf{H}^{\mathrm{s}} \delta \mathbf{m} \rangle \\ &\quad = \boldsymbol{\Sigma}^{\mathrm{sym}} \delta \overline{\mathbf{M}}^{\mathrm{sym}} \boldsymbol{\Sigma}^{\mathrm{sym}}. \end{aligned} \tag{3.17}$$

It can be shown $\langle \boldsymbol{\sigma} \mathbf{M}^{\mathrm{s}} \delta \boldsymbol{\sigma} \rangle = \langle \mathbf{m} \mathbf{H}^{\mathrm{s}} \delta \mathbf{m} \rangle = 0$, so that (3.17) can be simplified as:

$$c_r\langle \boldsymbol{\sigma} \delta \mathbf{M}_r^{\mathrm{s}} \boldsymbol{\sigma} + \mathbf{m} \delta \mathbf{H}_r^{\mathrm{s}} \mathbf{m} \rangle_r = \boldsymbol{\Sigma}^{\mathrm{sym}} \delta \overline{\mathbf{M}}^{\mathrm{sym}} \boldsymbol{\Sigma}^{\mathrm{sym}}. \tag{3.18}$$

Since $\delta \mathbf{M}_r^{\mathrm{s}}$ and $\delta \mathbf{H}_r^{\mathrm{s}}$ are independent, (3.18) leads naturally to (3.12a,b).

In summary, the proposed variational method is exactly equivalent to the secant moduli method based on the second-order stress and couple stress moments (Liu and Hu, in press). This variational method can be considered as the natural extension of Ponte Castañeda's variational method for a non-linear Cauchy medium, and the secant moduli interpretation of the latter has already been established by Suquet (1995) and Hu (1996). In the next section, this method will be applied to predict the non-linear behavior of selected non-linear micropolar composite systems subjected to either uniaxial or multiaxial loading.

## 4. Applications

Although the Hashin–Shtrikman bounds and self-consistent approximation of an incompressible composite with strain gradient effects have been provided by Smyshlyaev and Fleck (1994), as previously discussed, the strain gradient theory (Fleck and Hutchinson, 1993) they used is different from the micropolar theory used in this paper. At present, it appears that the bounds for a linear micropolar composite, like the Hashin–Shtrikman bounds for a Cauchy medium (Hashin and Shtrikman, 1963), are not available. The analytical estimate for the effective moduli of micropolar composites is only recently given by Sharma and Dasgupta (2002), Xun et al. (2004), Liu and Hu (in press). To apply the proposed variational method to a non-linear particle-reinforced micropolar composite and obtain analytical solutions, the particles are assumed to be elastic Cauchy medium, spherical in shape, randomly distributed, and have identical size with volume fraction $f$; the matrix material is taken as a non-linear micropolar medium that satisfies the power law of (2.19). According to Sharma and Dasgupta (2002) and Liu and Hu (in press), for a particulate composite, the effective moduli of the linear comparison

micropolar composite estimated by extending the Mori–Tanaka method (Mori and Tanaka, 1973) to a micropolar composite are given by:

$$\frac{\overline{\mu}^{s}}{\mu_0^{s}} = 1 + \frac{f}{(1-f)\beta^{s} + \mu_0^{s}/(\mu_1 - \mu_0^{s})}, \tag{4.1a}$$

$$\frac{\overline{K}^{s}}{K_0} = 1 + \frac{f}{(1-f)\alpha^{s} + K_0/(K_1 - K_0)}, \tag{4.1b}$$

where $(\overline{K}^{s}, K_1, K_0)$ are separately the bulk moduli of the linear comparison composite, particle, and matrix, $(\overline{\mu}^{s}, \mu_1, \mu_0^{s})$ are the corresponding shear moduli, and $(\beta^{s}, \alpha^{s})$ are the components of the average Eshelby tensor for the micropolar linear comparison matrix (Liu and Hu, in press):

$$\beta^{s} = \frac{6(K_0 + 2\mu_0^{s})}{5(3K_0 + 4\mu_0^{s})} - \frac{6\kappa_0}{5(\kappa_0 + \mu_0^{s})} G(\eta), \tag{4.2a}$$

$$\alpha^{s} = \frac{3K_0}{3K_0 + 4\mu_0^{s}}. \tag{4.2b}$$

Here, the superscript 's' represents quantities associated with the matrix of the linear comparison micropolar composite, and

$$G(\eta) = \mathrm{e}^{-\eta}(\eta^{-2} + \eta^{-3})[\eta\cosh\eta - \sinh\eta],$$

$$\eta = \frac{a}{h}, \quad h^2 = \frac{(\mu_0^{s} + \kappa_0)(\gamma_0^{s} + \beta_0^{s})}{4\mu_0^{s}\kappa_0},$$

where $a$ denotes the particle radius. Since $K_0$ and $\kappa_0$ are equal to their elastic counterparts, the superscript 's' has been dropped for these variables.

With (2.12) for the strain potential of a linear micropolar material and with the help from (3.18), we let $\mu_0^{s}$, $\beta_0^{s}$ and $\gamma_0^{s}$ have independent variations, resulting in:

$$\langle \sigma'_{(ij)}\sigma'_{(ij)}\rangle_0 = \frac{2}{3c_0}\left[\left(\frac{\mu_0^{s}}{\overline{\mu}^{s}}\right)^2 \frac{\partial\overline{\mu}^{s}}{\partial\mu_0^{s}}\Sigma_{\mathrm{e}}^2 + \frac{1}{3}\left(\frac{\mu_0^{s}}{\overline{K}^{s}}\right)^2 \frac{\partial\overline{K}^{s}}{\partial\mu_0^{s}}\overline{\Sigma}^2\right], \tag{4.3a}$$

$$\langle m'_{(ij)}m'_{(ij)}\rangle_0 = \frac{2}{3c_0}\left[\left(\frac{\beta_0^{s}}{\overline{\mu}^{s}}\right)^2 \frac{\partial\overline{\mu}^{s}}{\partial\beta_0^{s}}\Sigma_{\mathrm{e}}^2 + \frac{1}{3}\left(\frac{\beta_0^{s}}{\overline{K}^{s}}\right)^2 \frac{\partial\overline{K}^{s}}{\partial\beta_0^{s}}\overline{\Sigma}^2\right], \tag{4.3b}$$

$$\langle m_{\langle ij\rangle}m_{\langle ij\rangle}\rangle_0 = \frac{2}{3c_0}\left[\left(\frac{\gamma_0^{s}}{\overline{\mu}^{s}}\right)^2 \frac{\partial\overline{\mu}^{s}}{\partial\gamma_0^{s}}\Sigma_{\mathrm{e}}^2 + \frac{1}{3}\left(\frac{\gamma_0^{s}}{\overline{K}^{s}}\right)^2 \frac{\partial\overline{K}^{s}}{\partial\gamma_0^{s}}\overline{\Sigma}^2\right], \tag{4.3c}$$

where $\Sigma_{\mathrm{e}} = \sqrt{\frac{3}{2}\Sigma'_{(ij)}\Sigma'_{(ij)}}$, $\Sigma = \Sigma_{ii}$, and $\langle\bullet\rangle_0$ denotes the volume average of the said quantity over the matrix phase.

For the linear comparison micropolar composite, the effective stress of the matrix defined by (2.15) can now be written as:

$$\overline{\sigma}_{\mathrm{e}}^2 = A^2\Sigma_{\mathrm{e}}^2 + B^2\Sigma^2, \tag{4.4}$$

where $A$ and $B$ are non-dimensional parameters given by:

$$A^2 = \frac{\mu_0^{s^2}}{c_0\overline{\mu}^{s^2}}\left[\frac{\partial\overline{\mu}^{s}}{\partial\mu_0^{s}} + l_m^2\frac{\partial\overline{\mu}^{s}}{\partial\beta_0^{s}} + l_m^2\frac{\partial\overline{\mu}^{s}}{\partial\gamma_0^{s}}\right], \tag{4.5a}$$

$$B^2 = \frac{\mu_0^{s^2}}{3c_0\overline{K}^{s^2}}\left[\frac{\partial\overline{K}^{s}}{\partial\mu_0^{s}} + l_m^2\frac{\partial\overline{K}^{s}}{\partial\beta_0^{s}} + l_m^2\frac{\partial\overline{K}^{s}}{\partial\gamma_0^{s}}\right]. \tag{4.5b}$$

With the secant moduli given in (2.21) and the hardening law of (2.19), the elastic compliance of the linear comparison micropolar composite can now be determined as a function of the applied load. The corresponding strain and stress relation is given by (3.15), with the compliance tensor of the linear comparison micropolar composite $\overline{\mathbf{M}}^{\mathrm{sym}}$ expressed as:

$$\overline{\mathbf{M}}^{\mathrm{sym}}_{ijkl} = \frac{1}{4\overline{\mu}^{s}}(\delta_{ik}\delta_{jl} + \delta_{jk}\delta_{il}) + \left(\frac{1}{\overline{K}^{s}} - \frac{3}{2\overline{\mu}^{s}}\right)\delta_{ij}\delta_{kl}, \tag{4.6}$$

where the effective secant moduli $(\overline{K}^{s}, \overline{\mu}^{s})$ of the composite are related to constituent properties by (4.1). By setting $\overline{\sigma}_{\mathrm{e}} = \sigma_{\mathrm{y}}$ and let the elastic moduli of the linear comparison matrix equal the elastic moduli of the matrix phase of the actual composite, the initial yielding surface of the composite can be obtained. When the micropolar effect is neglected or $a \gg l_m$, the above formulation reduces to that obtained with the traditional Cauchy medium approach (Hu, 1997).

The general yielding criterion $\overline{\sigma}_{\mathrm{e}} = \sigma_{\mathrm{y}}$ will be applied below to selected metal matrix composite systems. For simplicity, only the initial yielding

of the composite will be considered. In general, the yield stress of the composite $\Sigma^y$, normalized by $\sigma_y$, can be written as:

$$\frac{\Sigma^y}{\sigma_y} = g(\tilde{\mu}, \tilde{k}, \rho, v, \eta, f). \tag{4.7a}$$

where $\tilde{\mu} = \frac{\mu_1}{\mu_0}$, $\tilde{k} = \frac{K_1}{K_0}$, $\rho = \frac{\kappa_0}{\mu_0}$, $v = \frac{K_0}{\mu_0}$, $\eta$ and $f$ are all non-dimensional parameters. Note that the influence of particle size is included in the parameter $\eta$, which is in turn related to the intrinsic length scale $l_m$ of the micropolar matrix:

$$\eta = \frac{a}{h} = \frac{a}{l_m}\sqrt{\frac{2\rho}{1+\rho}}. \tag{4.7b}$$

(a) General particulate composites

From Eqs. (4.5a,b) and the expressions for the effective moduli of the composite, (4.1a,b), we get:

$$A^2 = \frac{a_1 + a_2 G + a_3 G^2 + a_4 \eta G'}{\left[(1+\rho)((8+9v)(1-f(1-\tilde{\mu})) + 12\tilde{\mu} + 6v\tilde{\mu}) + 6\rho(1-f)(1-\tilde{\mu})(4+3v)G\right]^2}, \tag{4.8a}$$

$$B^2 = \frac{4f(1-\widetilde{k})^2}{[4-4f(1-\widetilde{k}) + 3v\widetilde{k}]^2}, \tag{4.8b}$$

where $G' \equiv \mathrm{d}G/\mathrm{d}\eta$, and

$$a_1 = (1+\rho)^2[6f(16+16v+9v^2)(1-\tilde{\mu})^2 + (8+9v+12\tilde{\mu}+6v\tilde{\mu})^2],$$

$$a_2 = 6\rho(4+3v)(1-\tilde{\mu})[2(1+\rho)(8+9v+12\tilde{\mu}+6v\tilde{\mu}) - f(1-\tilde{\mu})(16+18v-\rho(4-3v))],$$

$$a_3 = 36(1-f)\rho^2(4+3v)^2(1-\tilde{\mu})^2,$$

$$a_4 = -15f\rho(4+3v)^2(1-\tilde{\mu})^2.$$

The initial yield surface of the composite can then be written as

$$A^2\Sigma_e^2 + B^2\Sigma^2 - \sigma_y^2 = 0, \tag{4.9}$$

which reveals, in a simple and explicit manner, the size dependence of the initial yielding of a particulate composite. In the limit $\eta \to \infty$, $G \to 0$ and $\eta G' \to 0$, the results are independent of the parameter $\rho$ and reduce to those associated with the classical size-independent Cauchy composites (Hu, 1997), namely:

$$A^2 = \frac{6f(16+16v+9v^2)(1-\tilde{\mu})^2 + (8+9v+12\tilde{\mu}+6v\tilde{\mu})^2}{((8+9v)(1-f(1-\tilde{\mu})) + 12\tilde{\mu} + 6v\tilde{\mu})^2}, \tag{4.10}$$

with $B$ still given by (4.8b).

(b) Voids in elastically incompressible matrix

In this case, by letting $\tilde{\mu} = 0$, $\widetilde{k} = 0$ and $v \to \infty$, we have:

$$A^2 = \frac{(1+\rho)^2(3+2f) + 2\rho[6(1-f) + \rho(6-f)]G + 12\rho^2(1-f)G^2 - 5f\rho\eta G'}{3(1-f)^2(1+\rho+2\rho G)^2}, \tag{4.11a}$$

$$B^2 = \frac{f}{4(1-f)^2}. \tag{4.11b}$$

It is straightforward to check that when $\eta \to \infty$, $G \to 0$ and $\eta G' \to 0$, $A^2 = (1+2f/3)/(1-f)^2$, whatever values of $\rho$. This is the exact result corresponding to the case of voids surrounded by an incompressible Cauchy matrix (Hu, 1997).

(c) Rigid particle-reinforced elastically incompressible matrix composite

In this case, $\tilde{k} \to \infty$, $\tilde{\mu} \to \infty$ and $v \to \infty$, resulting in:

$$A^2 = \frac{2(1+\rho)^2(2+3f) - 6\rho[4+6f+\rho(4+f)]G + 36\rho^2(1-f)G^2 - 15f\rho\eta G'}{[(1+\rho)(2+3f) - 6\rho(1-f)G]^2}, \tag{4.12a}$$

$$B^2 = 0. \tag{4.12b}$$

Again, it is easy to check that when $\eta \to \infty$, $G \to 0$ and $\eta G' \to 0$, $A^2 = 1/(1+3f/2)$, which is the exact result for a rigid particle-reinforced elastically incompressible matrix Cauchy composite (Hu, 1997).

To check the predictive capability of the proposed method against available experimental results, several particulate composites are considered below, with the matrix taken as a non-linear micropolar medium and the particles as a linear elastic Cauchy medium.

Consider first a $Al_2O_3$–Al composite system subjected to uniaxial tension, for which the corresponding experimental results are given by Kouzeli and Mortensen (2002). The material constants used in the modeling and taken from Kouzeli and Mortensen (2002) are listed in Table 2. For higher-order material constants of the matrix, $\kappa = \mu/2$ and $l_m = 4.2$ μm are assumed; these values can give a better fit to the experimental results as shown shortly. The corresponding non-dimensional material parameters for the $Al_2O_3$–Al composite system are $\tilde{\mu} = 6.52$, $\tilde{k} = 3.71$, $\rho = 0.6$, and $v = 2.61$. Although at present there is no available experiment data to guide the selection of micropolar material constants, their values ought to lie in a reasonable range, and have the same order of magnitude as those obtained from material science approaches. For typical ductile metals the plasticity length scales of local non-uniform plastic deformation determined from the strain-gradient theory is indeed on the order of micrometers (see, e.g., Fleck et al., 1994; Gao et al., 1999a,b). Our choice of $l_m = 4.2$ μm for aluminum is consistent with this result.

The predicted uniaxial stress versus strain curves for the $Al_2O_3$–Al composite system with different particle sizes and volume fractions are plotted in Fig. 4 together with those measured by Kouzeli and Mortensen (2002). A total of four composite samples are examined, with the particle diameter $2a$ and volume fraction $f$ separately given by: (4.5 μm, 0.39), (9.3 μm, 0.54), (29.2 μm, 0.461)

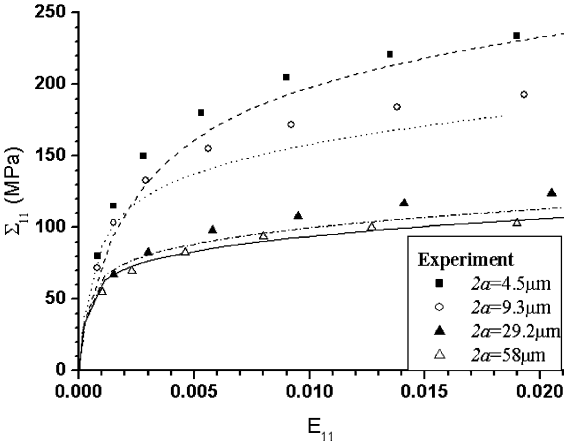


Fig. 4. Uniaxial tensile stress–strain curves of $Al_2O_3$–Al composite system: comparison between theory and experiment (Kouzeli and Mortensen, 2002).

Table 2
Material constants for $Al_2O_3$–Al composite system (Kouzeli and Mortensen, 2002)

| | $\mu$ (GPa) | $K$ (GPa) | $\kappa$ (GPa) | $l_m$ (μm) | $\sigma_y$ (MPa) | $h$ (MPa) | $n$ |
|---|---|---|---|---|---|---|---|
| Al | 25 | 65.2 | 12.5 | 4.2 | 25 | 110 | 0.255 |
| $Al_2O_3$ | 163.0 | 241.3 | | | | | |

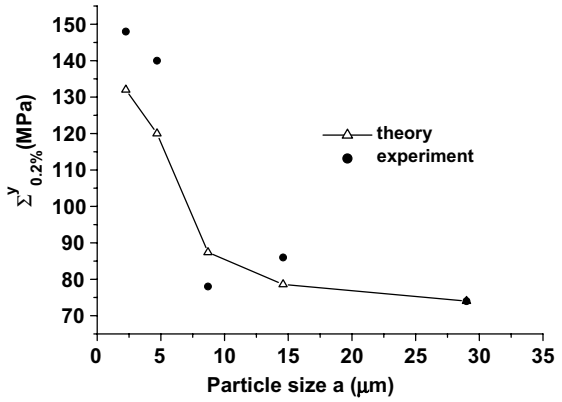


Fig. 5. Tensile yield stress (at 0.2% offset strain) of $Al_2O_3$–Al composite system plotted as a function of particle size: comparison between theory and experiment (Kouzeli and Mortensen, 2002).

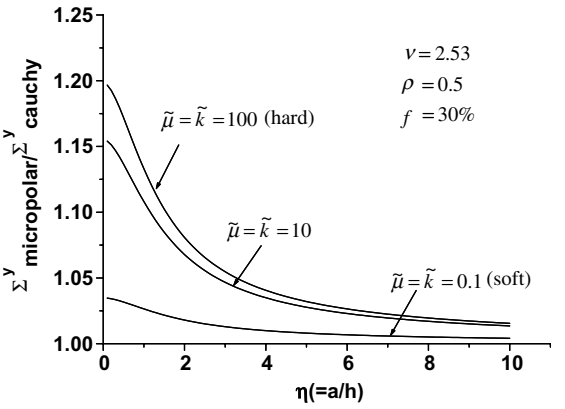


Fig. 6. Normalized initial yield stress of particulate composites plotted as a function of relative particle size $\eta(=a/h)$ for $v=2.53$, $\rho=0.5$ and $f=0.3$.

and (58 μm, 0.475). It is seen from Fig. 4 that an excellent correlation exists between the modeling and experiment over a large range of macroscopic strain.

Next, the predicted yield stress at 0.2% permanent strain as a function of particle radius $a$ is plotted in Fig. 5 together with that measured (Kouzeli and Mortensen, 2002). Again, close agreement is observed, although neither the predictions nor the experimental data exhibit smooth trend when the particle size is decreased. This is attributed to the fact that, whilst the particle size $a$ is varied, the particle volume fraction $f$ also varies for the composite samples tested by Kouzeli and Mortensen (2002). Fig. 6 plots the predicted uniaxial yield stress $\Sigma^y_{\text{micropolar}}$ (at 0.2% permanent strain) of the composite, normalized by that of the corresponding Cauchy composite $\Sigma^y_{\text{Cauchy}}$, as a function of relative particle size $\eta$ $(=a/h)$ for $v=2.53$, $\rho=0.5$ and $f=0.3$. The results show that for hard particle-reinforced composites, the strengthening effect is more pronounced when the particle size is reduced to the same level as the matrix intrinsic length, whereas for soft particle-reinforced composites, this size effect is much less significant.

Finally, based on Eqs. (4.4) and (4.5), the predicted initial yielding surfaces of different composite systems are plotted in Fig. 7. The results demonstrate how the deviatoric ($\Sigma_{\text{eff}}$) and hydrostatic ($\Sigma$) parts of the macroscopic stressing, normalized by the yielding stress of the matrix $\sigma_y$, would cause different composite systems to yield. The constants used in the computation for the micropolar matrix are $v=2.53$ and $\rho=0.5$, corresponding approximately to the aluminum matrix examined previously, whilst $\tilde{\mu}=10$ and $\tilde{k}=10$ are chosen for common particles. Two particle sizes are examined: $a=l_m$ and $a=100l_m$, corresponding to $\eta=0.82$ and $\eta=82$, respectively. In all the cases considered, the volume fraction of the particles is fixed at $f=0.3$.

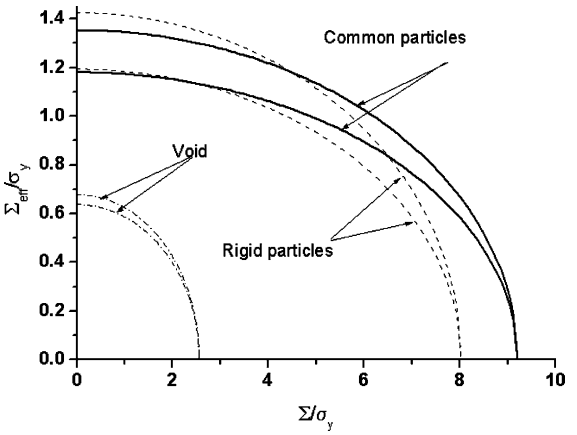


Fig. 7. Typical yield surfaces of particulate composites with size effects for $v=2.53$, $\rho=0.5$ and $f=0.3$.

It is seen from Fig. 7 that the size effect on initial yielding of a particulate composite is more

pronounced in shear loading and for hard particles. This is likely to be caused by the large fluctuations of stress and couple stress in the matrix for composites with hard particles and for composites loaded in shear. On the other hand, under hydrostatic loading, the model predicts no size effect for the composite, since in the micropolar theory, the local motion of the microstructure inside a material point is assumed to be rigid rotation, with the breathing-like (dilatation) deformation ignored (Eringen, 1999). The breathing-like deformation is believed to be more pronounced in porous matrix composites. To include this effect, a more refined higher-order continuum theory incorporating, for example, the microstretch theory needs to be used (see, e.g., Markov, 1981; Eringen, 1999; Liu and Hu, 2004). Correspondingly, at least two material length scales must be introduced, one to account for the rotation deformation, and the other for dilatation (Fleck and Hutchinson, 2001). However, for a polycrystal matrix such as aluminum, as demonstrated by the close agreement between theory and experiment in Figs. 4 and 5 the micropolar theory appears to be capable of capturing the nonlocal effect of the matrix when the particle size is comparable to the grain size and when the dilatation deformation is not dominant. The simplicity of the current approach and its capability to solve simple problems analytically compares favorably with other methods.

## 5. Conclusions

Ponte Castañeda's variational method has been extended from a non-linear Cauchy composite to a non-linear micropolar particulate composite. It is established that the micropolar version of Ponte Castañeda's variational method can be interpreted as the secant moduli method based on second-order stress and couple stress moments. The method is reduced to the classical micromechanic approach when the micropolar effect is neglected or the particle size is much larger than the intrinsic length scale of the matrix. With the deformation theory of micropolar plasticity having one intrinsic length scale adopted, it is demonstrated the influence of particle size on the yielding/strengthening and strain hardening of the composite can be taken into account in a simple and analytical manner. The predictions agree well with existing experiment results for particle-reinforced metal matrix composites, and it is found that the particle size effect is more pronounced in shear loading and for hard particles. Future work includes the extension of the micropolar theory to account for the dilatation effect that is important in void enlargement, indentation and crack-tip field studies.

## Acknowledgement

This work is supported partially by the National Natural Science Foundation of China under Grants no. 10325210 and 10332020, and partially by the State Scholarship Council of China for GKH's visit to Cambridge.

## References

Bassani, J.L., Needleman, A., Van der Giessen, E., 2001. Plastic flow in a composite: a comparison of nonlocal continuum and discrete dislocation predictions. Int. J. Solids Struct. 38, 833–853.

Budiansky, B., 1959. A reassessment of deformation theories of plasticity. J. Appl. Mech. 26, 259–263.

Chen, S., Wang, T.C., 2001. Strain gradient theory with couple stress for crystalline solids. Eur. J. Mech. A/Solids 20, 739–756.

Chen, S., Wang, T.C., 2002. Size effects in the particle-reinforced metal-matrix composites. Acta Mech. 157 (1–4), 113–127.

Christensen, R.M., Lo, K.H., 1979. Solutions for effective shear properties in three phase space and cylinder model. J. Mech. Phys. Solids 27, 315–330.

Eringen, A.C., 1968. Theory of micropolar elasticity. In: Leibowitz, H. (Ed.), Fracture, an Advanced Treatise. Academic Press, New York.

Eringen, A.C., 1999. Microcontinuum Field Theory. Springer.

Fleck, N.A., Hutchinson, J.W., 1993. A phenomenological theory for strain gradient effect in plasticity. J. Mech. Phys. Solids 41 (12), 1825–1857.

Fleck, N.A., Hutchinson, J.W., 2001. A reformulation of strain gradient plasticity. J. Mech. Phys. Solids 49, 2245.

Fleck, N.A., Muller, G.M., Ashby, M.F., Hutchinson, J.W., 1994. Strain gradient plasticity: theory and experiment. Acta Metall. Mater. 42, 475–487.

Forest, S., Dendievel, R., Canova, G.R., 1999. Estimating the overall properties of heterogeneous Cosserat materials. Modell. Simul. Mater. Sci. Eng. 7, 829–840.

Forest, S., Barbe, F., Cailletaud, G., 2000. Cosserat modeling of size effects in the mechanical behavior of polycrystals and muti-phase materials. Int. J. Solids Struct. 37, 7105–7126.

Gao, H., Huang, Y., Nix, W.D., 1999a. Modeling plasticity at the micrometer scale. Naturwissenschaften 86, 507–515.

Gao, H., Huang, Y., Nix, W.D., Hutchinson, J.W., 1999b. Mechanism-based strain gradient plasticity—I Theory. J. Mech. Phys. Solids 47, 1239–1263.

German, P., 1973. La methode des puissances virtuelles en mecanique des milieux continues premiere partie: theorie du second gradient. J. Mecanique 12, 235–273.

Haque, M.A., Saif, M.T.A., 2002. A novel technique for tensile testing of submicron scale freestanding specimens in SEM and TEM. Exp. Mech. 42 (1), 123–130.

Haque, M.A., Saif, M.T.A., 2003. Strain gradient effect in nanoscale thin films. Acta Mater. 51, 3053–3061.

Hashin, Z., Shtrikman, S., 1963. A variational approach to the theory of the elastic behavior of multiphase materials. J. Mech. Phys. Solids 11, 127–140.

Hori, M., Nemat-Nasser, S., 1993. Double-inclusion model and overall moduli of multi-phase composites. Mech. Mater. 14, 189–206.

Hu, G.K., 1996. A method of plasticity for general aligned spheroidal void or fiber-reinforced composites. Int. J. Plasticity 12, 439–449.

Hu, G.K., 1997. Composite plasticity based on matrix average second order stress moment. Int. J. Solids Struct. 34, 1007–1015.

Hu, G.K., Weng, G.J., 2000a. Connection between the double inclusion model and the Ponte Castañeda–Willis, Mori–Tanaka, and Kuster–Toksoz model. Mech. Mater. 32, 495–503.

Hu, G.K., Weng, G.J., 2000b. Some reflections on Mori–Tanaka and Ponte Castañeda–Willis and methods with randomly oriented ellipsoidal inclusions. Acta Mech. 140, 31–40.

Hu, G.K., Liu, X.N., Xun, F., 2004. Micromechanics of heterogeneous micropolar composite. Adv. Mech. 34, 95–214.

Jasiuk, I., Ostoja-Starzewski, M., 1995. Planar Cosserat elasticity of multiply-connected materials and intrusions. Appl. Mech. Rev. 48, S11–S18.

Ji, B., Wang, T.C., 2003. Plastic constitutive behavior of short-fiber/particle reinforced composites. Int. J. Plasticity 19, 565–581.

Koiter, W.T., 1964. Couple stresses in the theory of elasticity, I and II. Proc. Ned. Akad. Wet. (B) 67 (1), 17–43.

Kouzeli, M., Mortensen, A., 2002. Size dependent strengthening in particle reinforced aluminium. Acta Mater. 50, 39–51.

Kroner, E., 1958. Berechung der elastischen konstanten des vielkristalls aus den konstanten des einkristalls. Z. Phys. 151, 504–518.

Lippmann, H., 1995. Cosserat plasticity and plastic spin. ASME Appl. Mech. Rev. 48, 753–762.

Liu, X.N., Hu, G.K., in press. A continuum micromechanical theory of overall plasticity for particulate composites including particle size effect. Int. J. Plasticity.

Liu, X.N., Hu, G.K., 2004. Inclusion problem of microstretch continuum, Int. J. Engng. Sci. 42, 849–860.

Lloyd, D.J., 1994. Particle reinforced aluminum and magnesium matrix composites. Int. Mater. Rev. 39, 1–23.

Lubarda, V.A., Markenscoff, X., 2000. Conservation integrals in couple stress elasticity. J. Mech. Phys. Solids 48, 553–564.

Lubarda, V.A., Markenscoff, X., 2003. On conservation integrals in micropolar elasticity. Philos. Mag. A 83, 1365–1377.

Markov, K.Z., 1981. Dilatation theories of elasticity. ZAMM 61, 349–358.

Midlin, R.D., 1964. Microstructure in linear elasticity. Arch. Rational Mech. Anal. 16, 51–78.

Milton, G.W., 1981. Bounds on the electromagnetic, elastic and other properties of two-component composites. Phys. Rev. Lett. 46, 542–545.

Mori, T., Tanaka, K., 1973. Average stress in matrix and average elastic energy of materials with misfitting inclusions. Acta Metall. Mater. 21, 571–573.

Nemat-Nasser, S., Hori, M., 1993. Micromechanics: Overall Properties of Heterogeneous Materials. Elsevier, North-Holland.

Nowacki, W., 1986. Theory of Asymmetric Elasticity. Pergamon press.

Ponte Castañeda, P., 1991. The effective mechanical properties of nonlinear isotropic composite. J. Mech. Phys. Solids 39, 45–71.

Qiu, Y.P., Weng, G.J., 1992. A theory of plasticity for porous materials and particle-reinforced composites. Int. J. Plasticity 59, 261–268.

Sharma, P., Dasgupta, A., 2002. Average elastic field and scale-dependent overall properties of heterogeneous micropolar materials containing spherical and cylindrical inhomogeneities. Phys. Rev. B 66, 224110:1-10.

Smyshlyaev, V.P., Fleck, N.A., 1994. Bounds and estimates for linear composites with strain gradient effects. J. Mech. Phys. Solids 42, 1851–1882.

Smyshlyaev, V.P., Fleck, N.A., 1995. Bounds and estimates for the overall plastic behavior of composites with strain gradient effects. Proc. R. Soc. London A 451, 795–810.

Stölken, J.S., Evans, A.G., 1998. A microbend test method for measuring the plasticity length scale. Acta Mater. 42, 5109–5115.

Suquet, P., 1995. Overall properties of nonlinear composites: a modified secant moduli theory and its link with Ponte Castañeda's nonlinear variational procedure. C.R. Acad. Sci. Paris Ser. II 320, 563–571.

Tandon, G.P., Weng, G.J., 1988. A theory of particle-reinforced plasticity. ASME J. Appl. Mech. 55, 126–135.

Torquato, S., 1991. Random heterogeneous media: microstructure and improve bounds on effective properties. Appl. Mech. Rev. 44, 37–75.

Torquato, S., 2002. Random Heterogeneous Materials: Microstructures and Macroscopic Properties. Springer-Verlag, New York.

Toupin, R., 1962. Elastic materials with couple-stresses. Arch. Rational Mech. Anal. 11, 385–413.

Tsagrakis, I., Aifantis, E.C., 2002. Recent developments in gradient plasticity—Part I: Formulation and size effects; Part II: Plastic heterogeneity and vavelets. J. Eng. Mater. Technol. 124, 352–363.

Wang, N., Wang, Z., Aust, K.T., Erb, U., 1995. Effect of grain size on mechanical properties of nanocrystalline materials. Acta Mater. 43 (2), 519–528.

Wei, Y.G., 2001. Particulate size effects in the particle-reinforced metal-matrix composites. Acta Mech. Sinica 17 (1), 45–58.

Xue, Z., Huang, H., Li, M., 2002. Particle size effect in metallic materials: a study by the theory of mechanism-based strain gradient plasticity. Acta Mater. 50, 149–160.

Xun, F., Hu, G.K., Huang, Z.P., 2004. Effective in-plane moduli of composites with a micropolar matrix and coated fiber. Int. J. Solids Struct. 41, 247–265.

Yashin, H., Zbib, H.M., Khaleel, M.A., 2001. Size and boundary effects in discrete dislocation dynamics: coupling with continumm finite element. Mater. Sci. Eng. A 309–310, 294–299.

Zaoui, A., 2002. Continuum micromechanics: Survey. J. Eng. Mech.—ASCE 128 (8), 808–816.